

Sensing and atomic-scale structure analysis of single nuclear spin clusters in diamond

Fazhan Shi¹, Xi Kong¹, Pengfei Wang¹, Fei Kong¹, Nan Zhao², Ren-Bao Liu³,
Jiangfeng Du^{1*}

¹*National Laboratory for Physics Sciences at the Microscale and Department of Modern Physics, University of Science and Technology of China, Hefei, 230026, China*

²*Beijing Computational Science Research Center, Beijing 100084, China*

³*Department of Physics and Centre for Quantum Coherence, The Chinese University of Hong Kong, Shatin, New Territories, Hong Kong, China*

Single-molecule nuclear magnetic resonance (NMR) is a crown-jewel challenge in the field of magnetic resonance spectroscopy and has important applications in chemical analysis and in quantum computing. Recently, it becomes possible to tackle this grand challenge thanks to experimental advances in preserving quantum coherence of nitrogen-vacancy (NV) center spins in diamond as a sensitive probe¹⁻⁴ and theoretical proposals on atomic-scale magnetometry via dynamical decoupling control⁵. Through decoher-

*e-mail: djf@ustc.edu.cn

ence measurement of NV centers under dynamical decoupling control, sensing of single ^{13}C at nanometer distance has been realized⁶⁻⁸. Toward the ultimate goal of structure analysis of single molecules, it is highly desirable to directly measure the interactions within single nuclear spin clusters. Here we sensed a single ^{13}C - ^{13}C nuclear spin dimer located about 1 nm from the NV center and characterized the interaction between the two nuclear spins, by measuring NV center spin decoherence under various dynamical decoupling control. From the measured interaction we derived the spatial configuration of the dimer with atomic-scale resolution. These results demonstrate that central spin decoherence under dynamical decoupling control is a feasible probe for NMR structure analysis of single molecules.

In NMR, the structures of complex molecules can be unravelled by analysis of interaction between nuclear spins. Traditional magnetic resonance techniques rely on large ensembles of nuclear spins to accumulate signal-to-noise ratios. Recently, novel methods have been developed to improve the sensitivity including magnetic resonance force microscopy⁹ and optically detected magnetic resonance (ODMR)^{1-4, 10, 11}. Non-interacting single nuclear spins have been successfully sensed using NV center probes under dynamical decoupling control. However, measurement of interaction between nuclear spins within a single molecule and

resolving their structures are still challenging. Here we report experimental characterization of coherent coupling within a two-nuclear-spin cluster close to an NV center in diamond and determination of the cluster's spatial configuration using the interaction information.

The NV center consists of a nitrogen impurity and a neighbour vacancy. Its triplet ($S=1$) ground state can be spin-polarized and read out optically. It has ultra-long coherence time up to milliseconds in ultrapure samples¹² or under dynamical decoupling control¹³. These remarkable properties make the NV center a potential candidate for observing novel quantum phenomena^{14,15}, quantum processing^{16–26} and magnetic field sensing^{1,2}.

In pure diamond samples, NV center electron spins lose their coherence due to the magnetic fluctuation from surrounding ^{13}C nuclear spins. The fluctuation is dominated by single nuclear spin precession or flip-flop processes of spins clusters. Our measurement was carried out in strong field, where single spin precession was strongly suppressed²⁷, and therefore the interacting ^{13}C spin clusters are the dominant noise source. In this case, we are able to single out the physical effect caused by collective dynamics of nuclear spin clusters and, then, unravel the interaction within the cluster.

Among different kinds of ^{13}C nuclear spin clusters, a bonded ^{13}C spin dimer stands out because it can induce strong fingerprint modulations on NV center spin coherence⁵. In this work, we observed the dimer-induced modulation on NV center electron spin coherence, and characterized the interaction within the dimer and that between the dimer and the NV center electron spin.

In strong magnetic field, the dimer dynamics can be described by a pseudo-spin model, where the two-spin states $|\uparrow\downarrow\rangle$ and $|\downarrow\uparrow\rangle$ of the dimer are mapped to the spin-up $|\uparrow\rangle$ and spin-down $|\downarrow\rangle$ states of the pseudo-spin σ . The polarized dimer states $|\uparrow\uparrow\rangle$ and $|\downarrow\downarrow\rangle$ are energetically separated and irrelevant in the dynamics because of the large Zeeman energy in the strong field. The dynamics of the pseudo-spin is governed by the Hamiltonian⁵

$$H_{ps}^{(m_S)} = \frac{1}{2} \mathbf{h}^{(m_S)} \cdot \boldsymbol{\sigma} = \frac{1}{2} (X\sigma_x + Z^{(m_S)}\sigma_z), \quad (1)$$

where the component X of the pseudo-field $\mathbf{h}^{(\alpha)}$ is the nuclear dipolar interaction strength and the component $Z^{(m_S)}$ is due to the difference between hyperfine couplings of the two nuclei to the center spin, corresponding to the NV center electron spin state $|m_S\rangle$.

The pseudo-field component $Z^{(m_S)}$ and hence the nuclear spin pair dy-

namics depend on the NV center electron spin state $|m_S\rangle$. For the NV center spin in $|m_S = 0\rangle$ state, the hyperfine couplings vanish while for $|m_S = 1\rangle$ state, the hyperfine couplings of the two nuclear spins have a finite difference of $Z^{(1)} \sim 10$ kHz. Correspondingly the pseudo-spin will precess with frequencies $\omega_{\text{ps}}^{(0)} = X$ or $\omega_{\text{ps}}^{(1)} = \sqrt{X^2 + [Z^{(1)}]^2}$. When the NV center spin is prepared in a superposition state $(|m_S = 0\rangle + |m_S = 1\rangle) / \sqrt{2}$, the characteristic frequency of the noise induced by the pseudo-spin becomes $\omega_{\text{ps}}^{\text{eff}} = \sqrt{X^2 + \left[\frac{Z^{(1)}}{2}\right]^2}$ (SI, Sec. 1.2). In our experiment, the pseudo-spin precession frequency $\omega_{\text{ps}}^{\text{eff}}$ was measured by dynamical decoupling control^{13,28,29} of the NV center spin.

The setup and experimental scheme are schematically shown in Fig. 1. Carr-Purcell-Meiboom-Gill (CPMG) dynamical decoupling control sequences are employed to increase the sensitivity of the NV sensor. Figure 2 shows the NV center spin coherence under CPMG- N control. For pulse number $N > 4$, we observed coherence dips on top of smooth decoherence. The dip position t_{dip} is proportional to the pulse number N (Fig. 2b). In the intuitive picture (Fig. 1c), the transition in the ^{13}C dimer imposed an AC noise with a characteristic frequency. Therefore when the CPMG timing matches the noise characteristic frequency, the NV center spin decoherence was enhanced and therefore presented a dip^{5,8,30}. As shown in

previous works^{5,8}, the dip position is related to the precession frequency by

$$t_{\text{dip}} = \frac{N\pi}{\omega_{\text{ps}}^{\text{eff}}}, \quad (2)$$

from which we extracted the pseudo-spin precession frequency $\omega_{\text{ps}}^{\text{eff}} \approx 2\pi \times (7.3 \pm 0.1)$ kHz.

The pseudo-field components X and $Z^{(m_S)}$ were determined by comparing the observed dip widths and depths under various control pulse number N with the calculated electron spin coherence using the pseudo-spin model. Because the nuclear spin positions are discrete on diamond lattice, the dipolar interaction takes discrete values $X = 2.1$ kHz for a dimer in $[111]$ direction, $X = 0.685$ kHz for a dimer in other C-C bond directions, and $X < 0.3$ kHz for nuclear spins with larger distance. The calculation shows that only parameters $[X, Z^{(1)}] = [0.685, 14.6]$ kHz yield full agreement with the experiment data shown in Fig. 3. With this we conclude that the coherence dip was caused by a dimer along non- $[111]$ direction (SI, Sec. 3.1).

We characterized the coupling between the dimer and the NV center electron spin by measurement for various magnetic fields. The $Z^{(m_S)}$ component of the pseudo-field consists of two part $Z^{(m_S)} = Z_{\parallel}^{(m_S)} + Z_{\perp}^{(m_S)}(B_0)$. The parallel part

$Z_{\parallel}^{(m_S)} = A_{1,\parallel} - A_{2,\parallel}$ is the difference of the hyperfine fields projected to the applied magnetic field direction. The transverse part $Z_{\perp}^{(m_S)}(B_0) = \frac{(A_{1,\perp}^{(m_S)})^2 - (A_{2,\perp}^{(m_S)})^2}{\gamma_C B_0}$ comes from the perturbative frequency shifts of the two spins induced by virtual flipping via the polarized states $|\uparrow\uparrow\rangle$ and $|\downarrow\downarrow\rangle$ ²⁷. Notice that the parallel part is opposite for $|m_S = 1\rangle$ and $|m_S = -1\rangle$ states, but the transverse part is the same. The presence of the transverse part $Z_{\perp}^{(m_S)}(B_0)$ causes different dip positions for the transitions $|m_S = 0\rangle \leftrightarrow | + 1\rangle$ and $|m_S = 0\rangle \leftrightarrow | - 1\rangle$. The dip position difference δt_{dip} depends on the magnetic field. In the case of $Z_{\parallel}^{(m_S)} \gg Z_{\perp}^{(m_S)}(B_0)$, which is the case in our experiment,

$$\delta t_{\text{dip}} \approx \frac{2N}{(Z_{\parallel}^{(1)})^2} \frac{(A_{1,\perp})^2 - (A_{2,\perp})^2}{\gamma_C B_0}. \quad (3)$$

In the strong magnetic field limit, $\delta t_{\text{dip}} \rightarrow 0$, and $Z_{\parallel}^{(1)} = 14.6$ kHz is extracted from $\omega_{\text{ps}}^{\text{eff}}$, as shown in Fig.3 for $B = 1770$ Gauss. The magnetic field dependence of δt_{dip} gave the difference of the transverse hyperfine coupling $\delta A_{\perp}^2 = (A_{1,\perp})^2 - (A_{2,\perp})^2 = (21.7 \text{ kHz})^2$ (SI, Sec. 3.2). With the values of $Z^{(1)}$ and δA_{\perp}^2 , we determined the dimer was located about 1 nm away from the NV center (SI, Sec. 4). The field dependence of the dip features also excludes electron spin clusters as the cause of the coherent modulation (SI, Sec. 5).

In summary, we have observed and characterized nuclear spin interaction as

weak as 685 Hz within a single two-nuclear-spin cluster in diamond. By decoherence measurement of the NV center spin under multi-pulse dynamical decoupling control and various magnetic fields and by comparing the data with calculations, we determined the orientation, distance between the two nuclear spins, and distance from the NV center of the dimer, with atomic-scale resolution. These results demonstrate that the dynamical decoupling technique is promising for deriving the interaction between nuclear spins and therefore for structure analysis of single molecules on diamond surface using shallow NV centers.

Methods

The NV sensor in $\langle 100 \rangle$ face bulk diamond was mounted on a typical ODMR confocal setup which was synchronized together with the microwave bridge by multi-channels pulse generator (Spincore, PBESR-PRO-500). The nitrogen concentration was less than 5ppb and the abundance of ^{13}C was naturally equal to 1.1%. The pump 532nm green laser and phonon sideband fluorescence (wavelength, 650-800 nm) went through the same oil objective (Olympus, PLAPON 60XO, NA 1.42). Before the pump laser went into the objective, it was forced to go double through one AOM (ISOMET, power leakage ratio $\sim 1/1000$), to preserve T_1 of NV sensor from the leakage laser effect. Fluorescence inten-

sity, collected by avalanche photodiodes (Perkin Elmer, SPCM-AQRH-14) with a counter card, was used to monitor the magnetic signal on the NV sensor. The adjustable external magnetic field (0~2000 Gauss) created by the electrical coil (GMW model 5201, 3ppm/hour stability) was aligned by monitoring the diversification of fluorescence. Pulsed microwave was carried by a 20 μ m copper wire. The microwave phase was continuously adjusted by mechanical phase shifter and fixed to X and Y phase by network analyser (Agilent). High order CPMG- N sequences were used to amplify the weakly signal $Z^{(ms)}$ from remote nuclear spin pair, $Z^{(ms)} \sim \text{kHz} \ll \text{MHz} \sim 1/T_2^*$, in which, T_2^* was roughly 1 μ s in our sample. CPMG-12 on the different transitions $0 \leftrightarrow \pm 1$ under various magnetic field were employed to characterize the coupling vector and distinguish the high field threshold. Based on the experiment condition, the pseudo spin model was used to analyze the experiment result.

1. Balasubramanian, G. *et al.* Nanoscale imaging magnetometry with diamond spins under ambient conditions. *Nature* **455**, 648-651 (2008). [1](#), [2](#), [3](#)
2. Maze, J. R. *et al.* Nanoscale magnetic sensing with an individual electronic spin in diamond. *Nature* **455**, 644-647 (2008). [1](#), [2](#), [3](#)
3. Staudacher, T. *et al.* Nuclear magnetic resonance spectroscopy on a (5-

- nanometer)³ sample volume. *Science* **339**, 561-563 (2013). [1](#), [2](#)
4. Mamin, H. J. *et al.* Nanoscale nuclear magnetic resonance with a nitrogen-vacancy spin sensor. *Science* **339**, 557-560 (2013). [1](#), [2](#)
 5. Zhao, N., Hu, J. L., Ho, S. W., Wan, J. T. K. & Liu, R. B. Atomic-scale magnetometry of distant nuclear spin clusters via nitrogen-vacancy spin in diamond. *Nature Nanotech.* **6**, 242-246 (2011). [1](#), [4](#), [5](#), [6](#)
 6. Kolkowitz, S., Unterreithmeier, Q. P., Bennett, S. D. & Lukin, M. D. Sensing distant nuclear spins with a single electron spin. *Phys. Rev. Lett.* **109**, 137601 (2012). [2](#)
 7. Taminiau, T. H., Wagenaar, J. J. T., van der Sar, T., Jelezko, F., Dobrovitski, V. V. & Hanson, R. Detection and Control of Individual Nuclear Spins Using a Weakly Coupled Electron Spin. *Phys. Rev. Lett.* **109**, 137602 (2012). [2](#)
 8. Zhao, N. *et al.* Sensing single remote nuclear spins. *Nature Nanotech.* **7**, 657-662 (2012). [2](#), [5](#), [6](#)
 9. Degen, C. L., Poggio, M., Mamin, H. J., Rettner, C. T. & Rugar, D. Nanoscale magnetic resonance imaging. *Proc. Natl. Acad. Sci. USA* **106**, 1313-1317 (2009). [2](#)

10. Maletinsky, P. *et al.* A robust scanning diamond sensor for nanoscale imaging with single nitrogen-vacancy centres. *Nature Nanotech.* **7**, 320-324 (2012). [2](#)
11. Loretz, M. *et al.* Radio-frequency magnetometry using a single electron spin. *Phys. Rev. Lett.* **110**, 017602 (2013). [2](#)
12. Balasubramanian, G. *et al.* Ultralong spin coherence time in isotopically engineered diamond. *Nature Mat.* **8**, 383-387 (2009).
13. Ryan, C. A., Hodges, J. S. & Cory, D. G. Robust decoupling techniques to extend quantum coherence in diamond. *Phys. Rev. Lett.* **105**, 200402 (2010). [3](#), [5](#)
14. Huang, P. *et al.* Observation of an anomalous decoherence effect in a quantum bath at room temperature. *Nature Comm.* **2**, 570 (2011). [3](#)
15. Zhao, N., Wang, Z. & Liu, R. B. Anomalous decoherence effect in a quantum bath. *Phys. Rev. Lett.* **106**, 217205 (2011). [3](#)
16. Gaebel, T. *et al.* Room-temperature coherent coupling of single spins in diamond. *Nat. Phys.* **2**, 408-413 (2006). [3](#)
17. Dutt, M. V. G. *et al.* Quantum register based on individual electronic and nuclear spin qubits in diamond. *Science* **316**, 1312-1316 (2007). [3](#)

18. Neumann, P. *et al.* Multipartite entanglement among single spins in diamond. *Science* **320**, 1326-1329 (2008). [3](#)
19. Fuchs, G. D. *et al.* Gigahertz dynamics of a strongly driven single quantum spin. *Science* **326**, 1520-1522 (2009). [3](#)
20. Jiang, L. *et al.* Repetitive readout of a single electronic spin via quantum logic with nuclear spin ancillae. *Science* **326**, 267-272 (2009). [3](#)
21. Cappellaro, P., Jiang, L., Hodges, J. S. & Lukin, M. D. Coherence and control of quantum registers based on electronic spin in a nuclear spin bath. *Phys. Rev. Lett.* **102**, 210502 (2009). [3](#)
22. Neumann, P. *et al.* Quantum register based on coupled electron spins in a room-temperature solid. *Nat. Phys.* **6**, 249 (2010). [3](#)
23. Shi, F. Z. *et al.* Room-temperature implementation of the Deutsch-Jozsa algorithm with a single electronic spin in diamond. *Phys. Rev. Lett.* **105**, 040504 (2010). [3](#)
24. Xu, X. K. *et al.* Coherence-protected quantum gate by continuous dynamical decoupling in diamond. *Phys. Rev. Lett.* **109**, 070502 (2012). [3](#)

25. Sar T. V. D. *et al.* Decoherence-protected quantum gates for a hybrid solid-state spin register. *Nature* **82**, 484 (2012). [3](#)
26. Dolde, F. *et al.* Room-temperature entanglement between single defect spins in diamond. *Nat. Phys.* **9**, 139-143 (2013). [3](#)
27. Zhao, N., Ho, S. W. & Liu, R. B. Decoherence and dynamical decoupling control of nitrogen vacancy center electron spins in nuclear spin baths. *Phys. Rev. B* **85**, 115303 (2012). [3](#), [7](#)
28. Du, J. F. *et al.* Preserving electron spin coherence in solids by optimal dynamical decoupling. *Nature* **461**, 1265-1268 (2009). [5](#)
29. de Lange, G., Wang, Z. H., Riste, D., Dobrovitski, V. V. & Hanson, R. Universal dynamical decoupling of a single solid-state spin from a spin bath. *Science* **330**, 60-63 (2010). [5](#)
30. Lange, G. de., Riste, D., Dobrovitski, V. V., and & Hanson, R. Single-spin magnetometry with multipulse sensing sequences. *Phys. Rev. Lett.* **106**, 080802 (2011). [5](#)

Acknowledgements This work was supported by the National Key Basic Research Program of China (Grant No. 2013CB921800), the National Natural Science Foundation

of China (Grant Nos. 11227901, 91021005, 10834005, 11028510), the 'Strategic Priority Research Program (B)' of the CAS (Grant No. XDB01030400), the Fundamental Research Funds for the Central Universities, Hong Kong Research Grants Council (N_CUHK403/11, 402410 & HKU8/CRF/11G), the Chinese University of Hong Kong Focused Investments Scheme and 1000 Plan Program for Young Talents.

Author contributions J.D. and R.B.L. proposed the idea. J.D. and F.S. designed the experimental proposal. P.W., X.K. and F.S. prepared the experimental set-up. F.S., F.K. and X.K. performed the experiments. J.D. supervised the setup and experiments. N.Z. and F.S. carried out the calculation. F.S., N.Z., R.B.L. and J.D. wrote the paper. All authors analysed the data, discussed the results and commented on the manuscript.

Competing Interests The authors declare that they have no competing financial interests.

Additional information Supplementary information accompanies the paper on <http://www.nature.com/nnano>. Correspondence and requests for materials should be addressed to J.D.

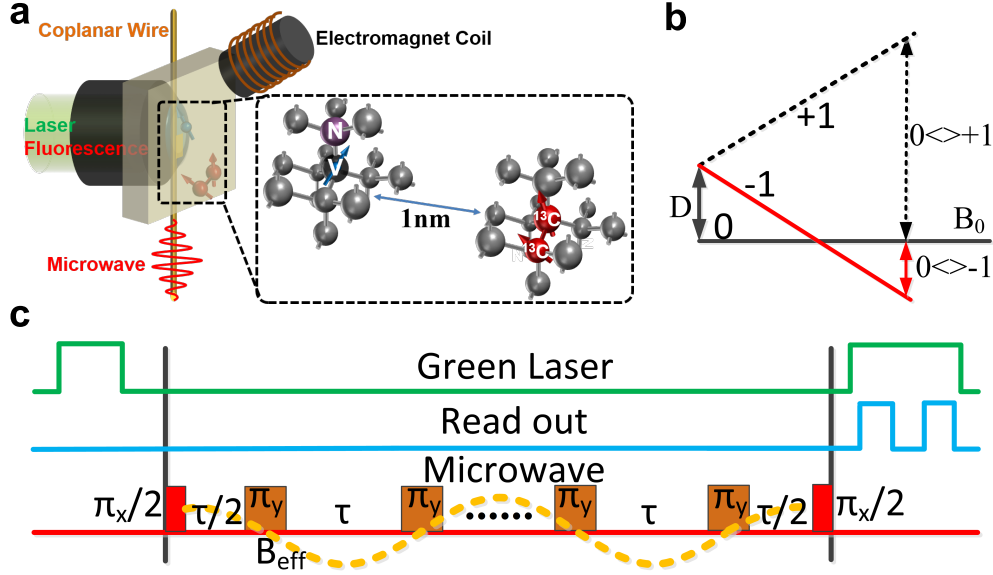


Figure 1: **Schematics of the setup and experimental methods.** (a) We measured the spin coherence of an NV sensor coupled to a ^{13}C - ^{13}C dimer. The external DC magnetic field was applied by a movable electric magnet while microwave was carried by a coplanar wire. (b) The degeneracy of the NV center spin states $|\pm 1\rangle$ was lifted by an external magnetic field B_0 along the NV axis. We encoded the quantum transition $0 \leftrightarrow -1$ (or $0 \leftrightarrow +1$) as a qubit and manipulated it by resonant microwave pulses. (c) The pulse sequences contained two green laser pulses for initialization and readout of the electron spin state and CPMG microwave pulses in between to control the spin.

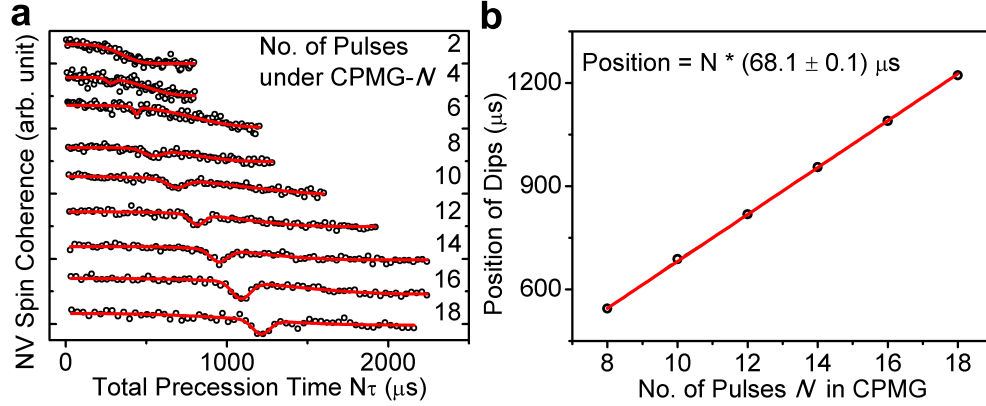


Figure 2: **Dip features in the NV center spin decoherence under CPMG control with various numbers of pulses.** (a) When the pulse number N of CPMG increased from 2 (top curve) to 18 (bottom curve), the dips induced by a spin dimer emerged and became more and more pronounced. The symbols are measured data and the curves are fitting by $\{y_0 + A_0 \exp[-(t/T_2)^4]\} \times \{y_1 + A_1 \exp[-2((t - t_c)/\omega)^2]/\omega/\sqrt{\pi/2}]\}$, which consists of a smooth profile and a Gaussian dip. (b) The position of the dips is proportional to the number of pulses in the CPMG control.

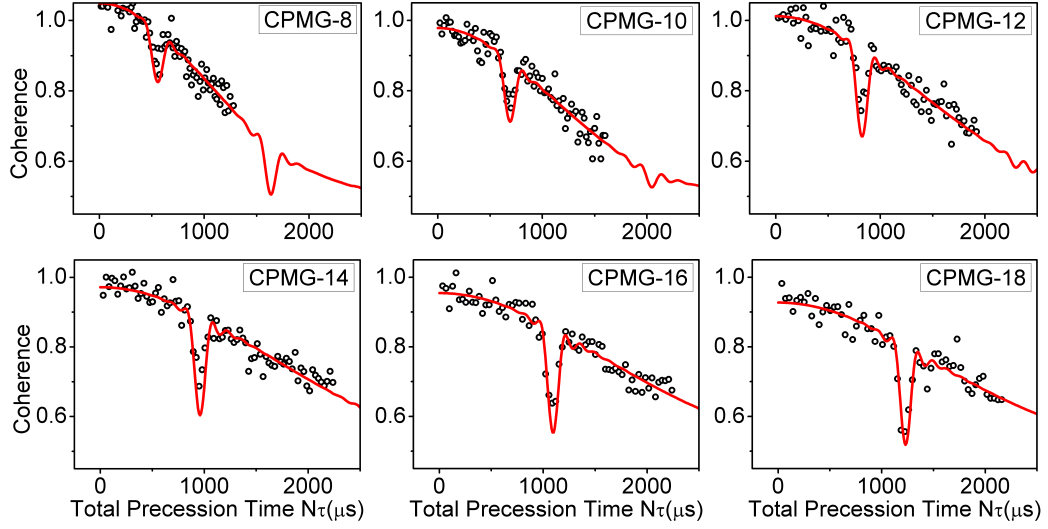


Figure 3: **Characterizing interaction of a nuclear spin dimer by fingerprint-matching between measurement and simulation.** The figures show NV spin coherence as a function of total evolution time of CPMG dynamical decoupling control with various number of pulses ($N=8, 10, 12, 14, 16$, and 18). The experimental data (symbols) are well reproduced by simulation (lines) based on a dimer with interaction $[X, Z^{(ms)}] = [0.685, 14.6]$ kHz. Other nuclear spin pairs do not produce dip features matching the experimental data. The magnetic field $B_0=1770$ G in the measurement.

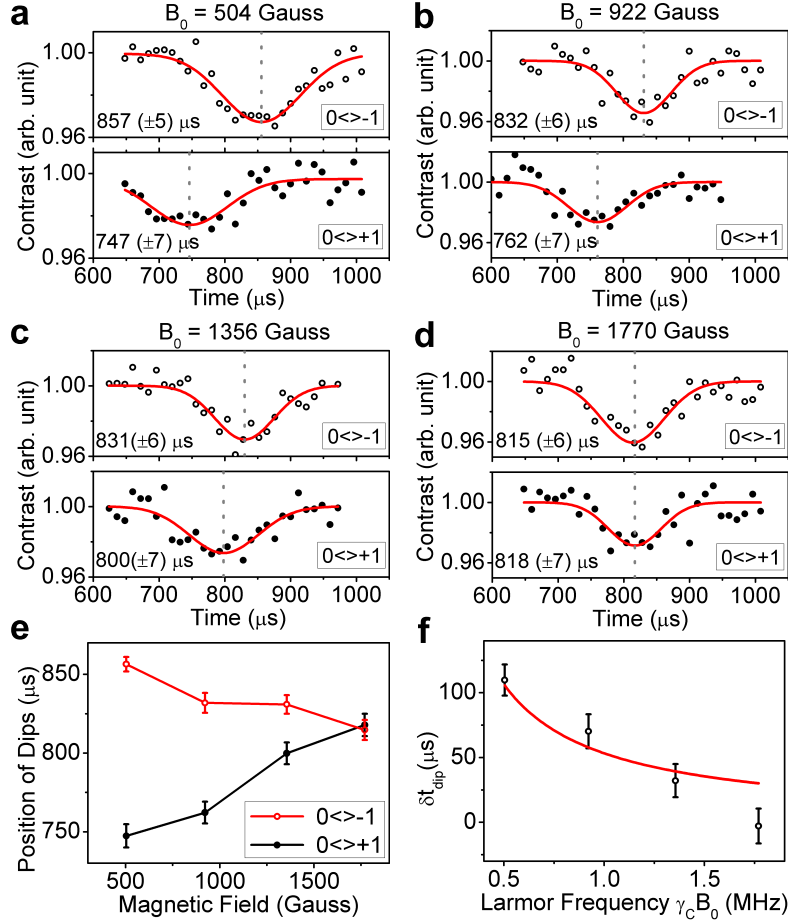


Figure 4: **Magnetic field dependence of the dip features for different transitions in the NV center spin decoherence.** (a-d) The upper and lower panels in each part show the CPMG-12 decoherence of the transitions $|0\rangle \leftrightarrow | +1\rangle$ and $|0\rangle \leftrightarrow |-1\rangle$, respectively. The magnetic field for (a)-(d) was in turn 504, 922, 1356, and 1770 Gauss. (e) Field dependence of the dip positions for different NV center spin transitions. (f) Comparison between the measured (symbols) and calculated (lines) positions of the dips as functions of the magnetic field.